



ORIGINAL ARTICLE

A sensitive and selective fluorescent probe for acetylcholinesterase: Synthesis, performance, mechanism and application



Meng Yao ^a, Hailiang Nie ^{a,*}, Wenxue Yao ^a, Xueping Yang ^a, Guowei Zhang ^{b,*}

^a Key Laboratory of Public Health Safety of Hebei Province, College of Public Health, Hebei University, Baoding 071002, Hebei, China

^b Hebei Collaborative Innovation Center of Tumor Microecological Metabolism Regulation, College of Traditional Chinese Medicine, Hebei University, Baoding 071002, Hebei, China

Received 16 November 2021; accepted 16 April 2022

Available online 22 April 2022

KEYWORDS

Acetylcholinesterase;
Fluorescent probe;
Rapid detection;
Pesticide poisoning

Abstract The detection of acetylcholinesterase (AChE) activity is of great significance for studying the physiological functions of AChE and clinical diagnosis of pesticide poisoning. Herein, a small-molecule fluorescent probe BDFA was rationally designed and readily synthesized via a one-step reaction, which enables qualitative and quantitative detection of AChE. BDFA emits a slight fluorescence in an aqueous medium, while the fluorescence is significantly enhanced under the catalysis of AChE. Mechanism studies reveal that BDFA eliminates the N, N-dimethyl carbamate protective group in the presence of AChE and then spontaneously undergoes intramolecular cyclization conversion to generate an intense fluorescent product. Based on the above mechanism, BDFA exhibits a sensitive, selective, rapid and stable “turn-on” fluorescence response to AChE, without interference from pH, ions, thiols, amino acids and other enzymes. The fluorescence intensity of BDFA at 525 nm has a linear relationship with the AChE concentration in the range of 0.0045–1.0 U/mL, and the detection limit is 4.5 mU/mL. Moreover, BDFA is suitable for rapidly diagnosing AChE activity in blood samples, thus providing an efficient and convenient tool for diagnosing organophosphorus and carbamate pesticide poisoning. Compared with the reported AChE fluorescent probes, BDFA exhibits apparent advantages including simple synthesis, low detection limit and fast response speed.

© 2022 The Author(s). Published by Elsevier B.V. on behalf of King Saud University. This is an open access article under the CC BY-NC-ND license (<http://creativecommons.org/licenses/by-nc-nd/4.0/>).

* Corresponding authors.

E-mail addresses: niehailiangts@163.com (H. Nie), xxzgw@126.com (G. Zhang).

Peer review under responsibility of King Saud University.



Production and hosting by Elsevier

1. Introduction

Cholinesterase (ChE) is a type of serine hydrolase produced by the liver, which mainly includes acetylcholinesterase (AChE) and butyrylcholinesterase (BChE). AChE specifically degrades acetylcholine into choline and acetic acid, and plays a vital role in maintaining the metabolic balance of acetylcholine (Koelle, 1962). Current studies

demonstrate that AChE has a variety of physiological functions, such as regulating nerve signal transmission (Wiesner et al., 2007), promoting nerve regeneration and participating in cell development and maturation (Johnson and Moore, 2006; Paraoanu and Layer, 2008). However, the function and metabolism of AChE are susceptible to severe disturbances from diseases such as hypertension, diabetes, asthma, Alzheimer's syndrome and liver damage (Ferreira-Vieira et al., 2016; Colovic et al., 2013; Wang et al., 2021). Moreover, the activity of AChE is significantly inhibited in the case of ingestion of organophosphorus and carbamate pesticides (King and Aaron, 2015), barbiturates (Mumtaz et al., 2013), and estrogen (Pereira et al., 2008). As a result, the determination of AChE activity is of great significance for studying the physiological functions of AChE and diagnosing AChE-related diseases.

The widely used methods for determining AChE activity mainly include Ellman's assay and ferric chloride spectrophotometry (Liu et al., 2021; Holas et al., 2012; Worek et al., 2012). The former method quantifies the AChE activity by measuring the concentration of thiocholine, a hydrolysis product under the catalysis of AChE, so it is susceptible to severe interference from biological thiols such as glutathione and cysteine (Yin et al., 2018; Yin et al., 2019; Yin et al., 2021). The latter method determines the AChE activity by measuring the residual concentration of the substrate acetylcholine, which has poor selectivity and requires colorimetric determination to be completed in a short time (Ellman et al., 1961; Beveridge et al., 1974). More seriously, the above two methods are essentially based on colorimetric measurement, which will inevitably be interfered by the inherent color of the sample matrix. The molecular-probe-based fluorimetric method has received extensive attention in detecting AChE due to its outstanding advantages in sensitivity, selectivity, rapid response, and portability (Xia et al., 2014). Although a large number of fluorescent probes for AChE have been reported, most of them require a secondary reaction to generate fluorescent signals (Feng et al., 2007; Fang et al., 2017; Meng et al., 2013; Wang et al., 2013; Arduini et al., 2013; Sun et al., 2011; Liao et al., 2013; Peng et al., 2009; Chang et al., 2016; Cui et al., 2011; Mertens et al., 2016), such as the nucleophilic reaction between the AChE hydrolysate thiocholine and the probe molecule (Peng et al., 2009; Chang et al., 2016; Cui et al., 2011; Mertens et al., 2016). These indirect measurements involve many analytical reagents and complex operation steps, and suffer from defects including low accuracy, poor repeatability and severe interference from sulfides. In 2019, inspired by the molecular structure of neostigmine (a well-known AChE inhibitor), Tang et al. designed a two-photon AChE-specific fluorescent probe (termed MCYN) using the N, N-dimethyl carbamate as the recognition group (Wang et al., 2019), which exhibits stronger fluorescence enhancement in the presence of AChE compared with BChE and other enzymes. After that, by using N, N-dimethyl carbamate as the recognition group, Guo, Lin, Yue and their research team synthesized near-infrared fluorescent probes for imaging AChE in cells and in vivo (Ma et al., 2020a, 2020b; He et al., 2021), and Yoon et al. developed a highly selective fluorescent probe specific for AChE by introducing a quaternary amine cation at the ortho position of the carbamate group (Wu et al., 2020). It is undeniable that these studies have significantly advanced the detection technology of AChE.

Despite extensive research, AChE fluorescence detection still needs breakthroughs in probe design and practical applications. As far as we know, only the five fluorescent probes mentioned above can directly sense AChE activity through a one-step reaction. These fluorescent probes usually require multi-step time-consuming synthesis and purification, severely limiting their practical applications. Herein, we reasonably designed a small-molecular fluorescent probe (B DFA), which enables the direct detection of AChE in water and serum (Fig. 1). B DFA with the N, N-dimethyl carbamate as the AChE recognition group was readily synthesized through a one-step reaction without complicated purification. In the presence of AChE, B DFA removes the carbamate group and then spontaneously undergoes an intramolecular cyclization reaction to produce a strong fluorescent product, thereby exhibiting a sensitive, selective, fast and stable fluo-

rescence reaction to AChE. Using B DFA as a fluorescent reagent, we successfully observed that the AChE activity in the blood was reduced after the introduction of organophosphorus and carbamate pesticides. Compared with the reported AChE fluorescent probes, B DFA shows obvious advantages including simple synthesis, low detection limit and fast response speed (Table S1).

2. Experimental section

2.1. Reagents and instruments

Dimethylcarbamic acid 2-formyl-5-(diethylamino) phenyl ester (BDFAM) was provided by Chemieliva Pharmaceutical Co., Ltd. 2-Benzothiazoleacetonitrile and other chemicals were commercially available from Innochem and used without further purification. Acetylcholinesterase (AChE, 200 U/g, extracted from electric eel), trypsin (TPS, 2500 U/mg), lysozyme (LZM, 2000 U/mg), bovine serum albumin (BSA, biotechnology grade), β -glucosidase (CB, 20 U/mg) were purchased from Macklin. Butyrylcholinesterase (BChE, 10 U/mg, extracted from horse serum) was purchased from Sigma-Aldrich. Ultrapure water (18.25 M Ω .cm, 25 °C) was used in all experiments.

NMR spectra were recorded on a Bruker Avance III spectrometer at 500 MHz for ¹H NMR and 125 MHz for ¹³C NMR. High-resolution mass spectrometry (HRMS) was measured on an Agilent 6520 Accurate-Mass Q-TOF LC/MS spectrometer. Fluorescence spectroscopic studies were performed on a Hitachi F-7000 spectrometer. Fluorescence decay dynamics were observed using an Edinburgh-Fluorescence Spectrometer FLS980 (Edinburgh, U.K.). UV-visible spectra were measured on a TU-1901 spectrometer.

2.2. Synthesis and characterization

Synthesis of B DFA: BDFAM (0.264 g, 1 mmol), 2-benzothiazoleacetonitrile (0.174 g, 1 mmol) and pyridine (2 drops) were dissolved in CH₃OH (30 mL) and stirred at room temperature for 8 h. Then, the solvent was removed under reduced pressure to produce a crude product, which was further purified by silica gel column chromatography (CH₃OH/CH₂Cl₂ = 1:20, v/v) to obtain B DFA as a yellow powder (21.0 mg, 0.5 mmol): yield 50%. ¹H NMR (500 MHz, Chloroform-*d*) δ 8.48 (d, *J* = 9.2 Hz, 1H), 8.25 (s, 1H), 8.00 (d, *J* = 8.2 Hz, 1H), 7.84 (d, *J* = 8.0 Hz, 1H), 7.47 (t, *J* = 7.7 Hz, 1H), 7.36 (t, *J* = 7.6 Hz, 1H), 6.60 (d, *J* = 9.2 Hz, 1H), 6.49 (s, 1H), 3.43 (q, *J* = 7.1 Hz, 4H), 3.28 (s, 3H), 3.08 (s, 3H), 1.23 (t, *J* = 7.1 Hz, 6H) (Fig. S4). ¹³C NMR (125 MHz, Chloroform-*d*) δ 165.07, 154.06, 153.91, 153.67, 151.92, 140.05, 134.47, 129.95, 126.50, 125.16, 123.06, 121.39, 118.01, 112.39, 109.25, 104.99, 98.17, 77.31, 77.06, 76.80, 44.88, 37.05, 36.75, 12.67 (Fig. S5). ESI-MS *m/z* calculated for [C₂₃H₂₄N₄O₂S + Na]⁺ 443.1512, measured 443.1517 (Fig. S6) Scheme 1.

Synthesis of the B DFA-AChE reaction product (BDFAP): B DFA (20 mg, 0.48 mmol) was fully dissolved in PBS solution (10 mM, pH = 7, containing 5% DMSO) and a sufficient amount of AChE was gradually added, and then the mixture was incubated at 37 °C for 40 min. The above solution was extracted with CH₂Cl₂ and the organic phase was concentrated under reduced pressure to obtain a crude product, which was

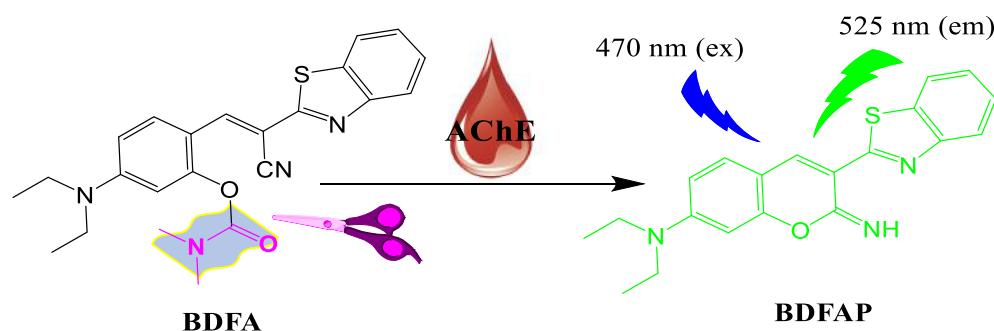
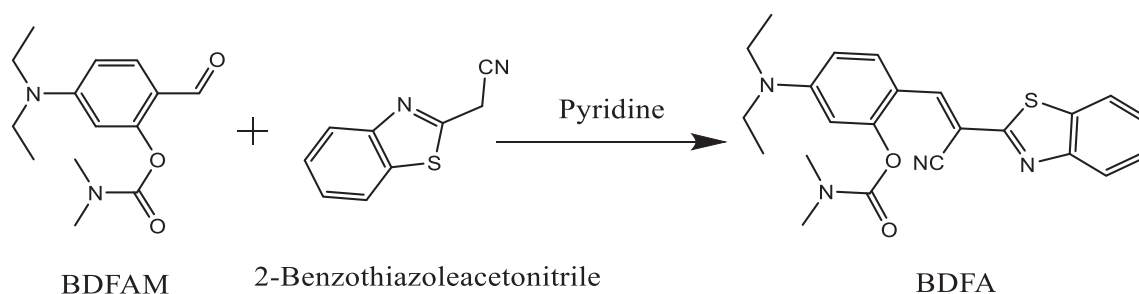


Fig. 1 Schematic diagram of the fluorescence response of BDFA to AChE.



Scheme 1 Synthetic route of BDFA.

further purified by silica gel column chromatography ($\text{CH}_3\text{-OH}/\text{CH}_2\text{Cl}_2 = 1:20$, v/v) to obtain BDFAP as a yellow powder. $^1\text{H NMR}$ (500 MHz, Methanol d_4) δ 8.16 (s, 1H), 8.00 (dd, $J = 15.4$, 8.0 Hz, 2H), 7.53 (t, $J = 7.7$ Hz, 1H), 7.44 (dt, $J = 7.7$, 3.2 Hz, 2H), 6.69 (dd, $J = 9.1$, 2.5 Hz, 1H), 6.53 (d, $J = 2.4$ Hz, 1H), 3.53 (q, $J = 7.1$ Hz, 4H), 1.26 (t, $J = 7.1$ Hz, 6H) (Fig. S7). ESI-MS m/z calculated for $[\text{C}_{20}\text{H}_{19}\text{-N}_3\text{OS} + \text{H}]^+$ 350.1322, measured 350.1320 (Fig. S8).

2.3. General procedures for fluorescence measurement

5 μL of BDFA stock solution (200 μM , DMSO) were added to the PBS solution (pH = 7.0, 10 mM), and then the stock solutions of various analytes were subsequently introduced. These analytes include: acetylcholinesterase (AChE, 10 U/mL), butyrylcholinesterase (BChE, 10 U/mL), glutamic acid (Glu, 10 mM), lysine (Lys, 10 mM), arginine (Arg, 10 mM), Tyrosine (Tyr, 10 mM), cysteine (Cys, 10 mM), tryptophan (Trp, 10 mM), glutathione (GSH, 10 mM), glucose (Glc, 10 mM), sucrose (Suc, 10 mM), dextran sulfate (DS, 10 mg/mL), trypsin (TPS, 400 U/mL), lysozyme (LZM, 100 U/mL), β -glucosidase (CB, 20 U/mL) and bovine serum albumin (BSA, 1 mg/mL). Subsequently, the above mixture was incubated at 37 $^\circ\text{C}$ for 40 min, and then its total volume was adjusted to 500 μL with a PBS solution (pH = 7.0, 10 mM). Finally, the solution was subjected to fluorescence measurement under excitation at 470 nm, with 900 V photomultiplier voltage and 5 nm excitation and emission bandwidth.

2.4. Molecular docking calculations

The molecular docking simulation was carried out on the software AutoDock 1.5.6. The crystal structure of AChE was

found in the protein data bank (PDB ID: 4bc1). The BDFA structure was optimized at the level of B3LYP/6-31G* on the solvation model of water by using Gaussian 09. The BDFA-AChE docking conformation was visualized using Pymol software, and its schematic diagram was also drawn using the same software.

2.5. Determination of AChE activity in blood

Blood samples collected from three healthy students in our laboratory were diluted 20 times with PBS solution (pH 7.0, 10 mM) to prevent blood clotting. The samples were divided into three parts. Two of which were added with Dichlorvos (final concentration: 100 $\mu\text{g}/\text{mL}$) and Carboway (final concentration: 100 $\mu\text{g}/\text{mL}$) and then incubated at room temperature for 30 min. Subsequently, the diluted blood (95 μL), pesticide-pretreated blood (95 μL) and PBS solution (95 μL) were added to BDFA (final concentration: 2 μM) in PBS solution (105 μL). The above mixture was incubated at 37 $^\circ\text{C}$ for 40 min, and finally fluorescence measurement was performed.

3. Results and discussion

3.1. Spectral response of BDFA to AChE

The optical properties of BDFA are closely related to its molecular configuration, which was first studied at the level of B3LYP/6-31G* on the solvation model of water using Gaussian 09. The results in Fig. 2a show that in the energy minimization configuration, the benzene ring and benzothiazole ring of BDFA are not distributed in a plane due to intramolecular steric hindrance, resulting in a distorted

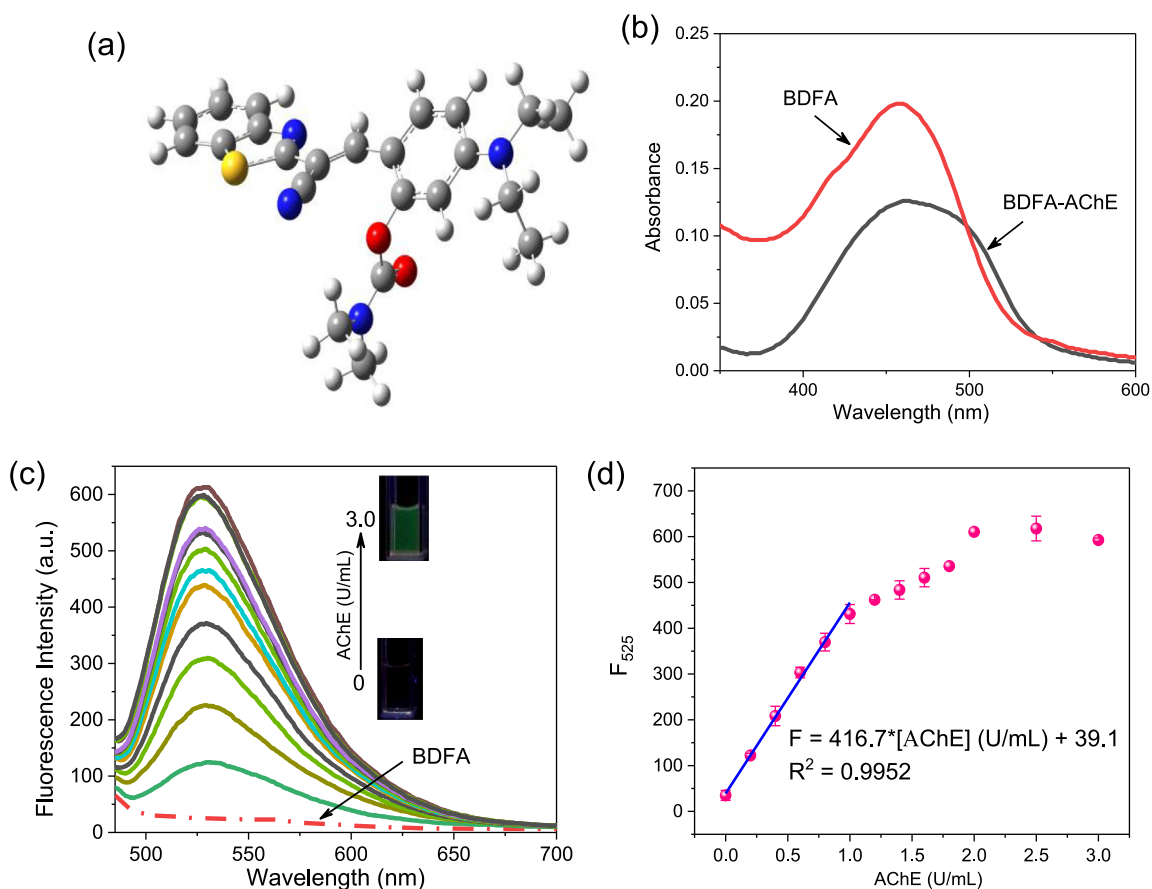


Fig. 2 (a) Energy-minimized conformation of BDFA. The white, gray, blue and yellow balls represent hydrogen, carbon, nitrogen and sulfur atoms, respectively. (b) Absorption spectra of BDFA (5 μM) in the absence and presence of AChE (3.0 U/mL). (c) Fluorescence spectra of BDFA (2 μM) and (d) its emission intensity at 525 nm varies with the AChE concentration in the range of 0–3.0 U/mL. All spectra were measured in PBS solution (pH 7.0, 10 mM) with excitation at 470 nm.

π -conjugated skeleton. Such non-planar structure is detrimental to fluorescence emission, and will reduce the background fluorescence from BDFA. In PBS solution, BDFA presents a main absorption band at 370–550 nm with a peak at 460 nm, which undergoes a noticeable enhancement and a small blue shift upon the addition of AChE (Fig. 2b). Under parallel conditions, BDFA emits weak fluorescence, which is consistent with the molecular configuration we simulated above. As an increasing concentration of AChE was introduced into the BDFA solution, a gradually enhanced emission centered at 525 nm appears, as shown in Fig. 2c. The fluorescence intensity at 525 nm rises sharply, and reaches a stable level after adding 2.0 U/mL AChE (Fig. 2d). The relationship between the fluorescence intensity at 525 nm and the AChE concentration in the range of 0.0045–1.0 U/mL conforms to the linear equation $F = 416.7 * [AChE] + 39.1$ ($R^2 = 0.9952$), and the detection limit (DL) was calculated as 4.5 mU/mL ($DL = 3\sigma/k$, where σ is the standard deviation (0.63) of the BDFA fluorescence intensity F_{525} in the absence of AChE under 11 parallel measurements, and k is the slope (416.7) of the linear equation plotting fluorescence intensity F_{525} vs AChE concentration). In general, BDFA exhibits a highly sensitive fluorescence response to AChE, which is expected to be applied to quantify AChE activity.

3.2. The selectivity of BDFA to AChE

To evaluate the selectivity in response to AChE, the fluorescence spectra of BDFA in the presence of various compounds were subsequently examined, and the results are shown in Fig. 3. It can be seen that the fluorescence shows an evident increase upon the addition of AChE or BChE, while other compounds, including common cations, anions, thiols, carbohydrates and enzymes only cause limited fluorescence changes. We also noticed that after adding the same concentration of AChE and BChE, the fluorescence intensity at 525 nm increases by 16.9 times and 5.2 times, respectively, which proves that the specificity of BDFA for AChE was much higher than that of BChE. Such results are consistent with the results of previous studies (Wang et al., 2019; Ma et al., 2020a, 2020b; He et al., 2021), which is speculated to be due to the better spatial match between the N, N-dimethyl carbamate group and the active cavity of AChE, thus causing the carbamate group to be easily hydrolyzed by AChE. Even in the coexistence of various compounds, BDFA still maintains a significant and relatively stable fluorescence response to AChE. The presence of BChE only increases the fluorescence response signal by 21%, so its interference is limited.

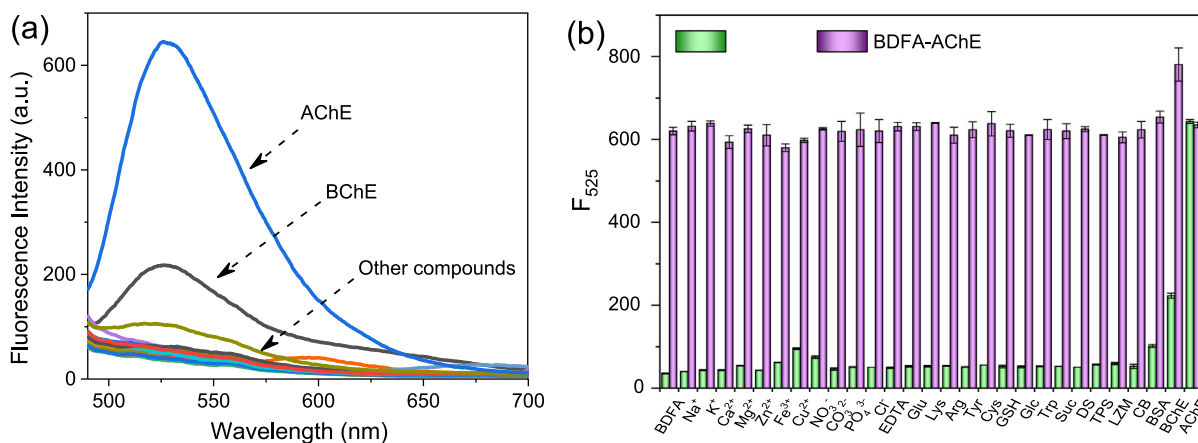


Fig. 3 (a) Fluorescence spectra of BDFA (2 μM) and (b) its emission intensity at 525 nm in the coexistence of various compounds, including Na⁺ (1 mM), K⁺ (1 mM), Ca²⁺ (1 mM), Mg²⁺ (1 mM), Zn²⁺ (1 mM), Fe³⁺ (1 mM), Cu²⁺ (1 mM), NO₃⁻ (1 mM), CO₃²⁻ (1 mM), PO₄³⁻ (1 mM), Cl⁻ (1 mM), EDTA (1 mM), Glu (1 mM), Lys (1 mM), Arg (1 mM), Tyr (1 mM), Cys (1 mM), GSH (1 mM), Trp (1 mM), GLC (1 mM), Suc (10 mM), DS (1 mg/mL), TPS (10 U/mL), LZM (10 U/mL), CB (10 U/mL), BSA (0.1 mg/mL), BChE (2.0 U/mL) and AChE (2.0 U/mL).

3.3. Response rate of BDFA to AChE

The BDFA-AChE reaction rate was studied by monitoring the dynamics of the fluorescence intensity over the reaction time. As displayed in Fig. 4a, BDFA emits extremely weak fluorescence, while the fluorescence gradually rises to a stable level within 20 min after adding AChE. Therefore, BDFA shows a fast response to AChE, which is suitable for rapidly detecting AChE activity.

3.4. pH effect

The effect of pH on the response of BDFA to AChE was subsequently evaluated. As shown in Fig. 4b and Fig. S1, the fluorescence of BDFA maintains a relatively stable level in the range of pH 5–10, and shows a significant and consistent response to AChE under neutral and weakly alkaline conditions (pH 7–9). These results indicate that BDFA is suitable for detecting AChE in near-neutral biological matrices such as blood and cytoplasm.

3.5. Impact of test time window on results

As shown in Fig. 4c, within 3 h, BDFA emits weak and stable fluorescence, while the BDFA-AChE reaction product only presents a small decrease in emission intensity. These results reveal that these two compounds have good time-dependent stability, providing a long-time window for reading the test results.

3.6. Response mechanism of BDFA to AChE

To explore the internal reaction mechanism, the BDFA-AChE molecular docking was simulated on Autodock software. The results in Fig. 5a reveal that there are multiple hydrophobic interactions and hydrogen bonds in the BDFA-AChE docking model, and the binding energy was calculated to be -8.53 Kcal/mol, suggesting that BDFA and AChE are spontaneously combined. As shown in Fig. 5b, the fluorescence decay kinetics of BDFA slows down slightly after reacting with AChE, and its average fluorescence lifetime increases from

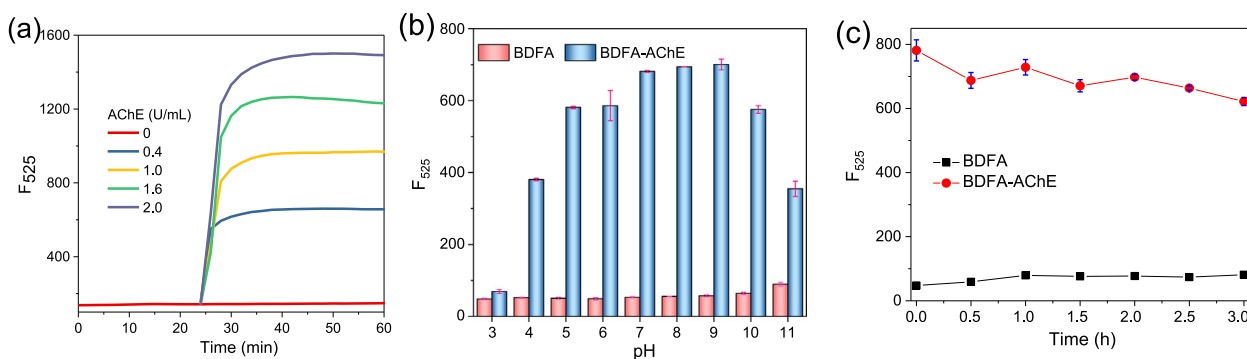


Fig. 4 (a) Time-dependent fluorescence intensity of BDFA (5 μM) after adding different concentrations (0, 0.4, 1.0, 1.6, 2.0 U/mL) of AChE. (b) Fluorescence intensity of BDFA (2 μM) in the absence and presence of AChE (2 U/mL) in PBS solutions of pH 3–11. (c) Changes in the fluorescence intensity of BDFA and BDFA-AChE reaction product with storage time. The fluorescence intensity was measured at 525 nm, with excitation at 470 nm.

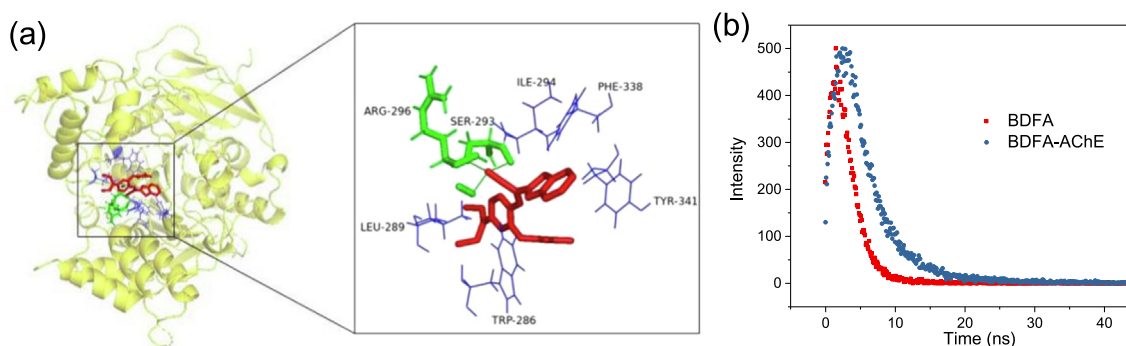


Fig. 5 (a) Molecular docking mode of BDFA and AChE. (b) Fluorescence decay kinetics of BDFA (5 μM) in the absence and presence of AChE (2.0 U/mL).

2.71 ns to 2.90 ns, indicating that a strong fluorescent compound may be produced.

To further clarify the reaction mechanism, we prepared and purified the BDFA-AChE reaction product (see section 2.2), and characterized its chemical structure by ^1H NMR (Fig. S6) and HRMS (Fig. S7). Moreover, we also performed a detailed analysis of the ^1H NMR spectra of BDFA and its reaction product with AChE (referred to as BDFAF) in Fig. 6a. It can be seen that the hydrogen atom signal (3.08 ppm, 3H; 3.28 ppm, 3H) attributed to the N, N-dimethyl carbamate group disappears in the NMR spectrum of BDFAP, confirming that the carbamate group is separated from the BDFA molecular under the catalysis of AChE. Fig. 6a also reveals an apparent redistribution of aromatic hydrogen atoms at 7.83–8.49 ppm, indicating that BDFAF has a different π -conjugated skeleton from BDFA. Concerning our previous and other studies (Cui et al., 2019; Zhang et al., 2021), we proposed the BDFA-AChE reaction mechanism, as described in Fig. 6b. First, the intramolecular ester bond of BDFA is hydrolyzed by AChE, which leads to the removal of the carbamate protecting group and produces an intermediate product (termed BDFAI). Subsequently, the phenolic hydroxyl group of BDFAI undergoes a nucleophilic reaction with its cyano group, causing an intramolecular cyclization reaction to generate the final product BDFAP with strong fluorescence emission. Our proposed mechanism for the BDFA-AChE reaction was also confirmed by the HPLC method (Fig. S3).

3.7. Determination of AChE activity in blood

Medical studies indicate that the AChE activity in serum can be used as a biomarker for detecting pesticide poisoning, assessing the severity of acute pancreatitis and predicting death (Xu et al., 2019; Badiou et al., 2008). Hence, we checked the feasibility of BDFA in detecting AChE activity in the serum matrix. As shown in Fig. 7, the fluorescence displays a significant increase after introducing the blood samples collected from three healthy individuals, demonstrating that the AChE in these samples maintains normal activity. As we all know, organophosphorus and carbamate pesticides severely inhibit the AChE activity due to the strong binding of pesticide molecules to the active sites of AChE (Bajjar, 2004). Therefore, we further monitored the changes in AChE activity of the blood samples in the presence of Dichlorvos and Carbaway (Guo et al., 2021). After adding the blood samples pre-incubated with the above two pesticides, the increase in fluorescence intensity is significantly reduced, indicating that the AChE activity in the blood samples is partially inhibited. These results confirm that BDFA is suitable for detecting AChE activity in blood matrix. In addition, we measured AChE activity in the blood samples using BDFA-based fluorometry and Ellman assay, a widely-used standard method for determining ChE activity. The detection results of the two methods are in good agreement (Table S2). The detected activities of AChE in the blood are also consistent with that in the literature (Xu et al., 2019).

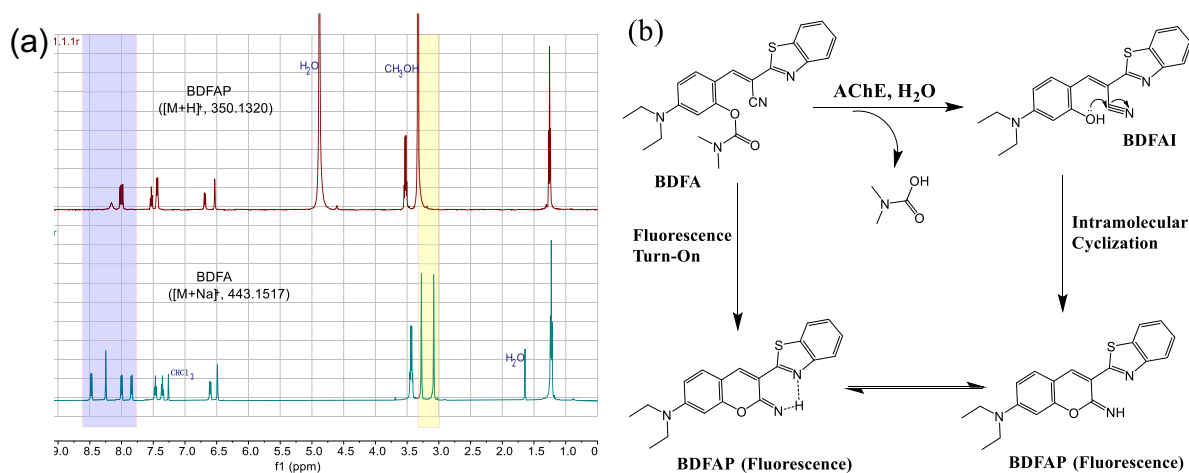


Fig. 6 (a) Comparison of the ^1H NMR spectra of BDFA and BDFAP. (b) Proposed reaction pathways for BDFA and AChE.

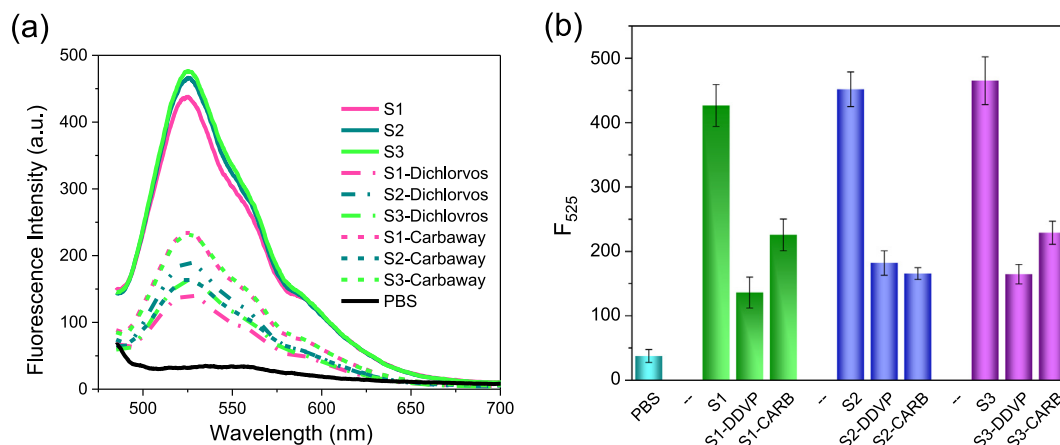


Fig. 7 (a) Fluorescence spectra and (b) emission intensity of BDFA (2 μM) upon the addition of PBS solution (pH 7.0, 10 mM), blood samples collected from three healthy individuals and these blood samples pre-treated with Dichlorvos (100 $\mu\text{g}/\text{mL}$) and Carboway (100 $\mu\text{g}/\text{mL}$).

4. Conclusion

In summary, we designed a small-molecule fluorescent probe BDFA, studied its performance for AChE analysis and explored the reaction mechanism. BDFA was readily synthesized through a one-step reaction without complicated purification. In the presence of AChE, BDFA exhibits a sensitive, selective, rapid and stable fluorescence enhancement, because the BDFA molecule eliminates the carbamate protecting group under the catalysis of AChE, and subsequently undergoes intramolecular cyclization conversion to generate a strong fluorescent product. An excellent linear relationship exists between the fluorescence intensity of BDFA and the concentration of AChE, and BDFA is suitable for the rapid detection of AChE activity in blood samples. Compared to the reported AChE fluorescent probes, BDFA shows apparent advantages in synthesis procedures, detection limit and response time. Our work provides an efficient and convenient tool for studying the physiological functions of AChE and diagnosing AChE-related diseases.

CRedit authorship contribution statement

Meng Yao: Methodology, Software, Formal analysis, Data curation. **Hailiang Nie:** Resources, Supervision, Writing – review & editing, Funding acquisition. **Wenxue Yao:** Formal analysis, Data curation. **Xueping Yang:** Methodology, Data curation. **Guowei Zhang:** Resources, Supervision, Funding acquisition.

Declaration of Competing Interest

The authors declare that they have no known competing financial interests or personal relationships that could have appeared to influence the work reported in this paper.

Acknowledgments

This work was supported by the Higher Education Science and Technology Research Project of Hebei Province (ZD2021009), the Health Family Planning Commission of Hebei Province (No. 20190123), Post-graduate's Innovation Fund Project of Hebei Province (cxzss2021018), Hebei Undergraduate Training Program for Innovation and Entrepreneurship (2021251),

National Undergraduate Training Program for Innovation and Entrepreneurship (2020390).

Appendix A. Supplementary material

Supplementary data to this article can be found online at <https://doi.org/10.1016/j.arabjc.2022.103929>.

References

- Arduini, F., Guidone, S., Amine, A., Paleschi, G., Moscone, D., 2013. Acetylcholinesterase biosensor based on self-assembled monolayer-modified gold-screen printed electrodes for organophosphorus insecticide detection. *Sens. Actuators, B* 179, 201–208. <https://doi.org/10.1016/j.snb.2012.10.016>.
- Badiou, A., Meled, M., Belzunces, L.P., 2008. Honeybee *Apis mellifera* acetylcholinesterase—a biomarker to detect deltamethrin exposure. *Ecotoxicol. Environ. Saf.* 69 (2), 246–253. <https://doi.org/10.1016/j.ecoenv.2006.11.020>.
- Bajgar, J., 2004. Organophosphates/nerve agent poisoning: mechanism of action, diagnosis, prophylaxis, and treatment. *Adv. Clin. Chem.* 38, 151–216. [https://doi.org/10.1016/s0065-2423\(04\)38006-6](https://doi.org/10.1016/s0065-2423(04)38006-6).
- Beveridge, T., Toma, S.J., Nakai, S., 1974. Determination of SS- and ss-groups in some food proteins using Ellman's reagent. *J. Food Sci.* 39 (1), 49–51. <https://doi.org/10.1111/j.1365-2621.1974.tb00984.x>.
- Chang, J., Li, H., Hou, T., Li, F., 2016. Paper-based fluorescent sensor for rapid naked-eye detection of acetylcholinesterase activity and organophosphorus pesticides with high sensitivity and selectivity. *Biosens. Bioelectron.* 86, 971–977. <https://doi.org/10.1016/j.bios.2016.07.022>.
- Colovic, M.B., Krstic, D.Z., Lazarevic-Pasti, T.D., Bondzic, A.M., Vasic, V.M., 2013. Acetylcholinesterase inhibitors. *Curr. Neuropharmacol.* 11 (3), 315–335. <https://doi.org/10.2174/1570159X11311030006>.
- Cui, J., Cao, L., Wang, G., Ji, W., Nie, H., Yang, C., Zhang, X., 2019. A fast-responding, highly sensitive detection system consisting of a fluorescent probe and palladium ions for N_2H_4 in environmental water and living cells. *Anal. Methods* 11 (39), 5023–5030. <https://doi.org/10.1039/C9AY01555H>.
- Cui, K., Chen, Z., Wang, Z., Zhang, G., Zhang, D., 2011. A naked-eye visible and fluorescence “turn-on” probe for acetylcholinesterase assay and thiols as well as imaging of living cells. *Analyst* 136 (1), 191–195. <https://doi.org/10.1039/c0an00456a>.

- Ellman, G.L., Courtney, K.D., Andres, V.J., Feather-Stone, R.M., 1961. A new and rapid colorimetric determination of acetylcholinesterase activity. *Biochem. Pharmacol.* 7, 88–95. [https://doi.org/10.1016/0006-2952\(61\)90145-9](https://doi.org/10.1016/0006-2952(61)90145-9).
- Fang, A., Chen, H., Li, H., Liu, M., Zhang, Y., Yao, S., 2017. Glutathione regulation-based dual-functional upconversion sensing-platform for acetylcholinesterase activity and cadmium ions. *Biosens. Bioelectron.* 87, 545–551. <https://doi.org/10.1016/j.bios.2016.08.111>.
- Feng, F., Tang, Y., Wang, S., Li, Y., Zhu, D., 2007. Continuous fluorometric assays for acetylcholinesterase activity and inhibition with conjugated polyelectrolytes. *Angew. Chem. Int. Ed. Engl.* 46 (41), 7882–7886. <https://doi.org/10.1002/anie.200701724>.
- Ferreira-Vieira, T.H., Guimaraes, I.M., Silva, F.R., Ribeiro, F.M., 2016. Alzheimer's disease: targeting the cholinergic system. *Curr. Neuropharmacol.* 14 (1), 101–115. <https://doi.org/10.2174/1570159X13666150716165726>.
- Guo, W.Y., Fu, Y.X., Liu, S.Y., Mei, L.C., Sun, Y., Yin, J., Yang, W. C., Yang, G.F., 2021. Multienzyme-Targeted fluorescent probe as a biosensing platform for broad detection of pesticide residues. *Anal. Chem.* 93 (18), 7079–7085. <https://doi.org/10.1021/acs.analchem.1c00553>.
- He, N., Yu, L., Xu, M., Huang, Y., Wang, X., Chen, L., Yue, S., 2021. Near-infrared fluorescent probe for evaluating the acetylcholinesterase effect in the aging process and dietary restriction via fluorescence imaging. *J. Mater. Chem. B* 9 (11), 2623–2630. <https://doi.org/10.1039/D0TB02833A>.
- Holas, O., Musilek, K., Pohanka, M., Kuca, K., 2012. The progress in the cholinesterase quantification methods. *Expert Opin. Drug Discovery* 7 (12), 1207–1223. <https://doi.org/10.1517/17460441.2012.729037>.
- Johnson, G., Moore, S.W., 2006. The peripheral anionic site of acetylcholinesterase: structure, functions and potential role in rational drug design. *Curr. Pharm. Design* 12 (2), 217–225. <https://doi.org/10.2174/138161206775193127>.
- King, A.M., Aaron, C.K., 2015. Organophosphate and carbamate poisoning. *Emerg. Med. Clin. N. Am.* 33 (1), 133–151. <https://doi.org/10.1016/j.emc.2014.09.010>.
- Koelle, G.B., 1962. A new general concept of the neurohumoral functions of acetylcholine and acetylcholinesterase. *J. Pharm. Pharmacol.* 14 (1), 65–90. <https://doi.org/10.1111/j.2042-7158.1962.tb11057.x>.
- Liao, D., Chen, J., Zhou, H., Wang, Y., Li, Y., Yu, C., 2013. In situ formation of metal coordination polymer: a strategy for fluorescence turn-on assay of acetylcholinesterase activity and inhibitor screening. *Anal. Chem.* 85 (5), 2667–2672. <https://doi.org/10.1021/ac302971x>.
- Liu, D., Xu, B., Dong, C., 2021. Recent advances in colorimetric strategies for acetylcholinesterase assay and their applications. *TrAC, Trends Anal. Chem.* 142, 116320. <https://doi.org/10.1016/j.trac.2021.116320>.
- Ma, J., Si, T., Yan, C., Li, Y., Li, Q., Lu, X., Guo, Y., 2020a. Near-infrared fluorescence probe for evaluating acetylcholinesterase activity in PC12 cells and In situ tracing AChE distribution in Zebrafish. *ACS Sensors* 5 (1), 83–92. <https://doi.org/10.1021/acssensors.9b01717>.
- Ma, Y., Gao, W., Ma, S., Liu, Y., Lin, W., 2020b. Observation of the elevation of cholinesterase activity in brain glioma by a near-infrared emission chemsensor. *Anal. Chem.* 92 (19), 13405–13410. <https://doi.org/10.1021/acs.analchem.0c02770>.
- Meng, X., Wei, J., Ren, X., Ren, J., Tang, F., 2013. A simple and sensitive fluorescence biosensor for detection of organophosphorus pesticides using H₂O₂-sensitive quantum dots/bi-enzyme. *Biosens. Bioelectron.* 47, 402–407. <https://doi.org/10.1016/j.bios.2013.03.053>.
- Mertens, M.D., Bierwisch, A., Li, T., Gutschow, M., Thiermann, H., Wille, T., Elsinghorst, P.W., 2016. A novel fluorogenic probe for the investigation of free thiols: application to kinetic measurements of acetylcholinesterase activity. *Toxicol. Lett.* 244, 161–166. <https://doi.org/10.1016/j.toxlet.2015.10.012>.
- Mumtaz, S., Hussain, R., Rauf, A., Fatmi, M.Q., Bokhari, H., Oelgemöller, M., Qureshi, A.M., 2013. Synthesis, molecular docking studies, and in vitro screening of barbiturates/thiobarbiturates as antibacterial and cholinesterase inhibitors. *Med. Chem. Res.* 23 (6), 2715–2726. <https://doi.org/10.1007/s00044-013-0847-2>.
- Paraoanu, L.E., Layer, P.G., 2008. Acetylcholinesterase in cell adhesion, neurite growth and network formation. *FEBS J.* 275 (4), 618–624. <https://doi.org/10.1111/j.1742-4658.2007.06237.x>.
- Peng, L., Zhang, G., Zhang, D., Xiang, J., Zhao, R., Wang, Y., Zhu, D., 2009. A fluorescence “turn-on” ensemble for acetylcholinesterase activity assay and inhibitor screening. *Org. Lett.* 11 (17), 4014–4017. <https://doi.org/10.1021/ol9016723>.
- Pereira, R.T., Porto, C.S., Godinho, R.O., Abdalla, F.M., 2008. Effects of estrogen on intracellular signaling pathways linked to activation of muscarinic acetylcholine receptors and on acetylcholinesterase activity in rat hippocampus. *Biochem. Pharmacol.* 75 (9), 1827–1834. <https://doi.org/10.1016/j.bcp.2008.01.016>.
- Sun, J., Guo, L., Bao, Y., Xie, J., 2011. A simple, label-free AuNPs-based colorimetric ultrasensitive detection of nerve agents and highly toxic organophosphate pesticide. *Biosens. Bioelectron.* 28 (1), 152–157. <https://doi.org/10.1016/j.bios.2011.07.012>.
- Wang, F., Liu, X., Lu, C.H., Willner, I., 2013. Cysteine-mediated aggregation of Au nanoparticles: the development of a H₂O₂ sensor and oxidase-based biosensors. *ACS Nano* 7 (8), 7278–7286. <https://doi.org/10.1021/nn402810x>.
- Wang, X., Li, P., Ding, Q., Wu, C., Zhang, W., Tang, B., 2019. Observation of acetylcholinesterase in stress-induced depression phenotypes by two-photon fluorescence imaging in the mouse brain. *J. Am. Chem. Soc.* 141 (5), 2061–2068. <https://doi.org/10.1021/jacs.8b11414>.
- Wiesner, J.Í., K í, Z.K., Ku A, K., Jun, D., Ko A, J., 2007. Acetylcholinesterases - the structural similarities and differences. *J. Enzym. Inhib. Med. Ch.* 22 (4), 417–424. [10.1080/14756360701421294](https://doi.org/10.1080/14756360701421294).
- Wang, Z., Wu, Z., Zuo, G., Lim, S.S., Yan, H., 2021. Defatted seeds of oenothera biennis as a potential functional food ingredient for diabetes. *Foods* 10 (3), 538. <https://doi.org/10.3390/foods10030538>.
- Worek, F., Eyer, P., Thiermann, H., 2012. Determination of acetylcholinesterase activity by the Ellman assay: a versatile tool for in vitro research on medical countermeasures against organophosphate poisoning. *Drug Test. Anal.* 4 (3–4), 282–291. <https://doi.org/10.1002/dta.337>.
- Wu, X., An, J.M., Shang, J., Huh, E., Qi, S., Lee, E., Li, H., Kim, G., Ma, H., Oh, M.S., Kim, D., Yoon, J., 2020. A molecular approach to rationally constructing specific fluorogenic substrates for the detection of acetylcholinesterase activity in live cells, mice brains and tissues. *Chem. Sci.* 11 (41), 11285–11292. <https://doi.org/10.1039/d0sc04213g>.
- Xia, N., Wang, Q., Liu, L., 2014. Nanomaterials-based optical techniques for the detection of acetylcholinesterase and pesticides. *Sensors* 15 (1), 499–514. <https://doi.org/10.3390/s150100499>.
- Xu, X., Cen, Y., Xu, G., Wei, F., Shi, M., Hu, Q., 2019. A ratiometric fluorescence probe based on carbon dots for discriminative and highly sensitive detection of acetylcholinesterase and butyrylcholinesterase in human whole blood. *Biosens. Bioelectron.* 131, 232–236. <https://doi.org/10.1016/j.bios.2019.02.031>.
- Yin, G., Niu, T., Gan, Y., Yu, T., Yin, P., Chen, H., Zhang, Y., Li, H., Yao, S., 2018. A multi-signal fluorescent probe with multiple binding sites for simultaneous sensing of cysteine, homocysteine, and glutathione. *Angew. Chem., Int. Ed.* 57 (18), 4991–4994. <https://doi.org/10.1002/anie.201800485>.
- Yin, G., Niu, T., Yu, T., Gan, Y., Sun, X., Yin, P., Chen, H., Zhang, Y., Li, H., Yao, S., 2019. Simultaneous Visualization of endogenous homocysteine, cysteine, glutathione, and their transformation through different fluorescence channels. *Angew. Chem., Int. Ed.* 58 (14), 4557–4561. <https://doi.org/10.1002/anie.201813935>.

Yin, G., Gan, Y., Jiang, H., Yu, T., Liu, M., Zhang, Y., Li, H., Yin, P., Yao, S., 2021. Direct quantification and visualization of homocysteine, cysteine, and glutathione in Alzheimer's and Parkinson's disease model tissues. *Anal. Chem.* 93 (28), 9878–9886. <https://doi.org/10.1021/acs.analchem.1c01945>.

Zhang, Q., Fu, C., Guo, X., Gao, J., Zhang, P., Ding, C., 2021. Fluorescent determination of butyrylcholinesterase activity and its application in biological imaging and pesticide residue detection. *ACS Sensors* 6 (3), 1138–1146. <https://doi.org/10.1021/acssensors.0c02398>.